Intermediate depth warming in the tropical Atlantic related to weakened thermohaline circulation: Combining paleoclimate data and modeling results for the last deglaciation

Carsten Rühlemann,[1] Stefan Mulitza, Gerrit Lohmann, André Paul, Matthias Prange, and Gerold Wefer

Department of Geosciences and Research Center "Ocean Margins", University of Bremen, Bremen, Germany

Received 1 July 2003; revised 10 October 2003; accepted 25 November 2003; published 17 March 2004.

[1] Benthic foraminiferal oxygen isotope ratios from two sediment cores recovered at 426 and 1299 m water depth in the eastern and western tropical Atlantic show that a slowdown of the thermohaline circulation (THC) during Heinrich event H1 and the Younger Dryas was accompanied by rapid and intense warming of intermediate depth waters. Millennial-scale covariations of low paleosalinities in the subpolar North Atlantic with decreased benthic oxygen isotope ratios in the eastern tropical Atlantic throughout the past 10,000 years suggest that THC weakening might be related to middepth warming during the Holocene period as well. Climate model experiments simulating a strong reduction of the THC in the Atlantic Ocean under present-day and glacial conditions reveal that the increase of temperature in the middepth tropical and South Atlantic is a common feature for both climatic states, caused by a reduced ventilation of cold intermediate and deep waters in conjunction with downward mixing of heat from the thermocline. From the similarity of the paleoclimatic records with the model simulations, we infer that the characteristic pattern of temperature change in the Atlantic Ocean related to weakened thermohaline circulation can serve as an indicator of present-day and future THC slowdown. *INDEX TERMS:* 4231 Oceanography: General: Equatorial oceanography; 4255 Oceanography: General: Numerical modeling; 4267 Oceanography: General: Paleoceanography; 4532 Oceanography: Physical: General circulation; *KEYWORDS:* tropical Atlantic, intermediate depth water, thermohaline circulation

Citation: Rühlemann, C., S. Mulitza, G. Lohmann, A. Paul, M. Prange, and G. Wefer (2004), Intermediate depth warming in the tropical Atlantic related to weakened thermohaline circulation: Combining paleoclimate data and modeling results for the last deglaciation, *Paleoceanography*, *19*, PA1025, doi:10.1029/2003PA000948.

1. Introduction

[2] Millennial climate changes under glacial and interglacial conditions have been related to changes in the Atlantic meridional overturning circulation [e.g., *Bond et al.*, 1997, 2001; *Oppo et al.*, 2001, 2003]. In particular, the strong increase in atmospheric radiocarbon during the last two large abrupt climate events, Heinrich event H1 (16,000 years BP) and the Younger Dryas (12,000 years BP), indicates that these climate shifts were associated with massive reductions in the rate of the North Atlantic Deep Water (NADW) formation [*Hughen et al.*, 1998; *Clark et al.*, 2002], possibly triggered by iceberg or meltwater discharge into the northern North Atlantic [*Broecker*, 1994]. Paleodata and simulations with ocean-climate general circulation models point out that the shifts in thermohaline circulation (THC) strength involved a characteristic seesaw pattern of sea-surface temperature change. Caused by the massive decrease in the Atlantic northward heat transport, the surface northern North Atlantic cooled by up to several degrees Celsius, while the western tropical Atlantic and South Atlantic slightly warmed by up to $\sim$1°C [*Mix et al.*, 1986; *Charles et al.*, 1996; *Manabe and Stouffer*, 1997; *Arz et al.*, 1999; *Rühlemann et al.*, 1999; *Vidal et al.*, 1999; *Hüls and Zahn*, 2000]. Climate models furthermore predict a salient warming at intermediate depths for present climate conditions that can reach up to several degrees Celsius in the tropical latitudes [*Manabe and Stouffer*, 1997; *Rind et al.*, 2001]. However, none of the general circulation models used to study the temperature response to THC weakening has been conducted for present and past climate conditions (i.e., glacial insolation, ice sheet distributions, atmospheric greenhouse gases). Therefore it remains unclear whether the pronounced intermediate depth warming is a characteristic of THC slowdown for modern as well as for glacial climate conditions.

[3] Changes in the Atlantic THC might have also affected the climate of the relatively stable Holocene period. Paleoclimate records from high-latitude marine sediments show that the current interglacial interval was punctuated by several millennial-scale cooling events, albeit considerably weaker in amplitude than its glacial counterparts [*Bond et al.*, 1997, 2001]. High-resolution sediment records of sortable silt [*Bianchi and McCave*, 1999] and benthic

[1] Now at Bundesanstalt für Geowissenschaften und Rohstoffe, Referat Meeresgeologie, Hannover, Germany.

0883-8305/04/2003PA000948$12.00

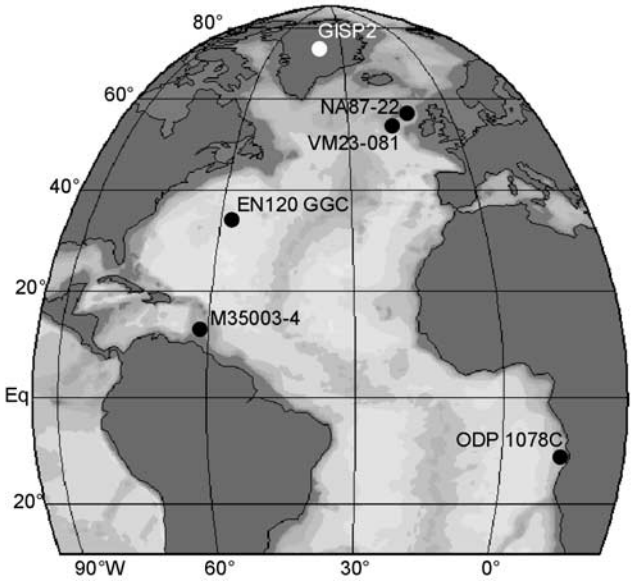

Figure 1. Locations of the studied sediment cores ODP 1078C and M35003-4 in the tropical Atlantic Ocean, the sediment cores EN120 GGC, VM23-081, and NA87-22 in the North Atlantic, and the Greenland GISP2 ice core.

foraminiferal carbon isotopes [*Oppo et al.*, 2003] suggest that these cooling events may have been related to changes in the rate of NADW formation. Unlike for high latitudes, little is known about Holocene millennial temperature changes in the low-latitude Atlantic [*deMenocal et al.*, 2000; *Poore et al.*, 2003] and its relation to changes in THC. Understanding this teleconnection of climate variability is particularly relevant because the meridional overturning circulation constitutes a major uncertainty in the prediction of future climate. On the basis of various climate modeling studies the Intergovernmental Panel on Climate Change (IPCC) anticipates that anthropogenic increases in atmospheric greenhouse gas concentrations will possibly cause a weakening or even a shutdown of the Atlantic THC through global heating and intensification of the hydrological cycle [*Cubasch et al.*, 2001]. For the early detection of THC weakening, it would thus be valuable to know the characteristic pattern of a concomitant ocean temperature change.

[4] In this study we investigate the ocean's temperature response to large changes in Atlantic northward heat transport, using model experiments and benthic foraminiferal oxygen isotope records from intermediate depths in the tropical Atlantic, covering the last 22,000 years. The isotope records and the model simulations consistently suggest that abrupt slowdowns of the THC during Heinrich event H1 and the Younger Dryas were accompanied by rapid and intense warming of intermediate depth tropical waters. Meltwater experiments with a three-dimensional ocean general circulation model running under present-day and glacial conditions show that this intermediate depth warming is a persistent feature of THC slowdown, independent from the climatic background state. We thus propose that the distinctive ocean temperature pattern associated with THC slowdown can help in tracing Holocene and possibly future THC changes.

2. Material and Methods

2.1. Site Locations

[5] The cores used in this study were located in the Tobago Basin, southeast of the island of Grenada on the Atlantic side of the Caribbean sill (M35003-4; 12°05′ N, 61°15′ W; 1299 m water depth), and off the coast of Angola (ODP 1078C; 11°55′ S, 13°24′ E; 426 m water depth) (Figure 1). Site M35003 is located in the transition zone between Antarctic Intermediate Water and Upper North Atlantic Deep Water, the two major contributors to the modern Atlantic intermediate depth circulation, and ODP Site 1078C is situated within the South Atlantic Central Water. Continuous influx of riverine suspension loads from the Orinoco and Amazon rivers in the western Atlantic causes enhanced average sedimentation rates of 15 cm per thousand years (15 cm kyr^{-1}) at core site M35003-4, whereas high average sedimentation rates of 55 cm kyr^{-1} at ODP site 1078C are due to resuspension of Angola shelf fine material (Figure 2).

2.2. Stable Oxygen Isotopes

[6] To reconstruct intermediate depth temperatures, we used the oxygen isotope composition of the epibenthic foraminifera *Cibicidoides wuellerstorfi* for the Caribbean core M35003-4, sampled at 5 cm intervals corresponding to ~310 years (Figure 2a; data are from *Hüls* [2000] provided through the PANGEA database; for replicate determinations of $\delta^{18}O$ at core depths 275, 280, 285, and 295 cm, we used the average values). Owing to the limited abundance of *C. wuellerstorfi* in ODP core 1078C, we employed the endobenthic species *Bolivina dilatata* for $\delta^{18}O$ measure-

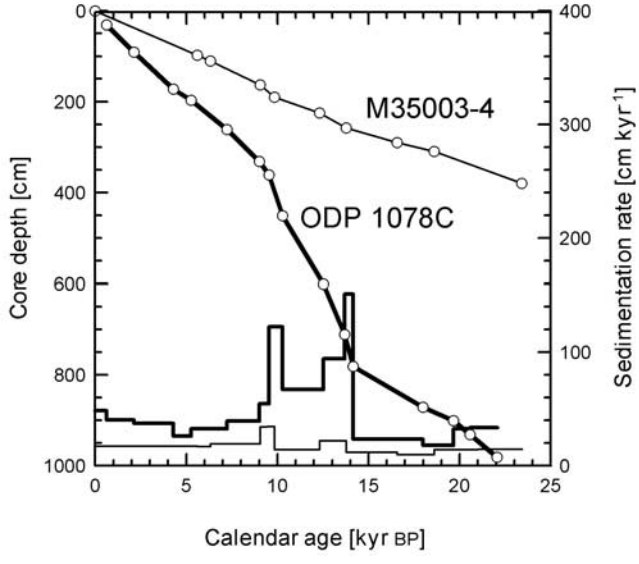

Figure 2. Age models for cores ODP 1078C and M35003-4 based on radiocarbon dates converted to calendar ages. Thick and thin lines at the bottom are sedimentation rates for cores ODP 1078C and M35003-4, respectively.

Table 1. ^{14}C Dates Used to Constrain the Age-Depth Model for ODP Core 1078C[a]

Laboratory ID	Core Section	Interval, cm	Composition Depth, cm bsf	^{14}C Age, years BP	± Error, years	Calendar Age, cal kyr BP	Analyzed Material
KIA13022	1H-1	30–32	31	1070	35	0.64	planktic forams, otholits
KIA13021	1H-1	90–92	91	2490	40	2.13	planktic forams
KIA16170	1H-2	22.5–24.5	173.5	4210	35	4.29	planktic forams
KIA16169	1H-2	47.5–49.5	198.5	4900	35	5.26	planktic forams
KIA13018	1H-2	110–112	261	6685	45	7.22	planktic forams, fractured mollusks
KIA13036	1H-3	30–32	331	8570	60	9.00	planktic forams, fractured mollusks
KIA13035	1H-3	60–62	361	8930	70	9.55	snail
KIA13017	1H-4	0–2	451	9520	70	10.28	mollusks
KIA13016	1H-5	0–2	601	10920	90	12.52	planktic forams, fractured mollusks
KIA13025[b]	2H-1	40–42	711	12110	90	13.74	fractured mollusks, scaphopods
KIA13014[b]	2H-1	40–42	711	12260	90	13.82	fractured mollusks, scaphopods
KIA13013	2H-1	110–112	781	12730	80	14.15	fractured mollusks
KIA13026	2H-2	50–52	871	15530	120	17.98	fractured mollusks
KIA13010	2H-2	80–82	901	16990	130	19.66	planktic forams
KIA13009	2H-2	110–112	931	17790	140	20.58	fractured mollusks
KIA13034[c]	2H-2	140–142	961	15780	120	18.26	fractured mollusks
KIA13032[c]	2H-3	0–2	971	16610	+130/−120	19.22	fractured mollusks
KIA13031	2H–3	10-12	981	19070	170	22.05	fractured mollusks

[a]Radiocarbon ages were determined on samples of mixed planktic foraminifera and mollusk fragments. The ^{14}C ages were converted to calendar ages using the program CALIB 4.3 and the marine data set [*Stuiver et al.*, 1998].
[b]These two samples were averaged to determine the calendar age for 711cm sediment depth.
[c]Not used for the age model.

ments at this core site (Figure 2a). *B. dilatata* is a shallow infaunal species typical for low-oxygen environments of the upper continental slope [*Schmiedl et al.*, 1997]. The δ^{18}O values of this species are similar to that of epibenthic species [*Dunbar and Wefer*, 1984] so that *B. dilatata* can be used to infer ambient bottom-water oxygen isotope composition and temperature variation. The δ^{18}O record of ODP core 1078C was measured at 2.5 cm sampling space, equivalent to an average resolution of ~60 years. Bulk sediment samples were washed over 150- and 63-μm sieves and dried in an oven at 60°C for faunal analysis. From each sample, 15–30 specimens of *B. dilatata* (350–400 μm) were picked out for isotope analyses. The isotopic composition of the foraminiferal shells was measured using a Finnigan MAT 251 mass spectrometer equipped with an automatic carbonate preparation device and reported against VPDB. Internal precision, based on replicates of a limestone standard, was better than ±0.07‰.

2.3. Stratigraphy

[7] The stratigraphy for core M35003-4 is based on 10 accelerator mass spectrometry (AMS) ^{14}C datings for the past 23,500 years (23.5 kyr) [*Rühlemann et al.*, 1999; *Hüls and Zahn*, 2000] and for ODP core 1078C on 16 AMS^{14}C datings for the past 22 kyr (Table 1). The ^{14}C ages were converted into a calendar year age scale using the CALIB conversion routine [*Stuiver and Reimer*, 1993; *Stuiver et al.*, 1998] with the marine data set.

[8] Age control is of key importance when estimating rates of change and correlating records across the Atlantic. This is particularly critical for the Younger Dryas and Heinrich 1 events when the THC weakening may have caused an increase in surface water reservoir age (R_{surf}) of 100–200 years in the tropical Atlantic [*Stocker and Wright*, 1996] compared to the modern values of ~400 years [*Bard*, 1988]. Past R_{surf} may have differed from today, but only sparse data exist. For the western tropical Atlantic, varved sediments from the Cariaco Basin in the southern Caribbean Sea (430 km SW of core site M35003-4) suggest that the present-day R_{surf} of 420 years did not change between 11.5 and 9 cal kyr BP [*Hughen et al.*, 1998]. Millennial changes in R_{surf} of more than ~100 years before 11.5 cal kyr are also unlikely given the limited variability of the tropical R_{surf} between the end of the Pleistocene and the present [*Stuiver et al.*, 1998]. Possible changes of R_{surf} at the eastern Atlantic region of core site ODP 1078C are not documented, but recent freshwater experiments with the LSG ocean general circulation model suggest that changes of the regional ^{14}C reservoir age during the Younger Dryas and Heinrich event H1 are in the order of a few decades compared to a glacial value of 600 years [*Butzin et al.*, 2003]. In summary, we have no evidence for changes in R_{surf} of more than a few hundred years during the last deglaciation and the Holocene at either core site.

[9] Continuous timescales for both cores were obtained by linear interpolations between the age control points (Figure 2). Core M35003-4 shows an almost linear age-depth relationship and constant sedimentation rates, indicating a relatively continuous supply of fine suspension to the core site. The age-depth relationship of ODP core 1078C exhibits a steepening between 14 and 9 kyr, a period of increased sea level rise [*Fairbanks*, 1989] when the rapid flooding of the African shelf led to intensified erosion and downslope transport of terrigenous particles causing enhanced sedimentation rates.

2.4. Model Setup and Experimental Design

[10] Here we use the Bremen Earth system model of intermediate complexity (BREMIC) [*Lohmann et al.*, 2003]. The ocean model component is based on the Hamburg large-scale geostrophic model LSG [*Maier-Reimer et al.*, 1993]. The horizontal resolution is 3.5° on a semi-staggered grid (type "E") with 11 levels in the vertical. A third-order QUICK scheme [*Leonard*, 1979; *Schäfer-Neth*

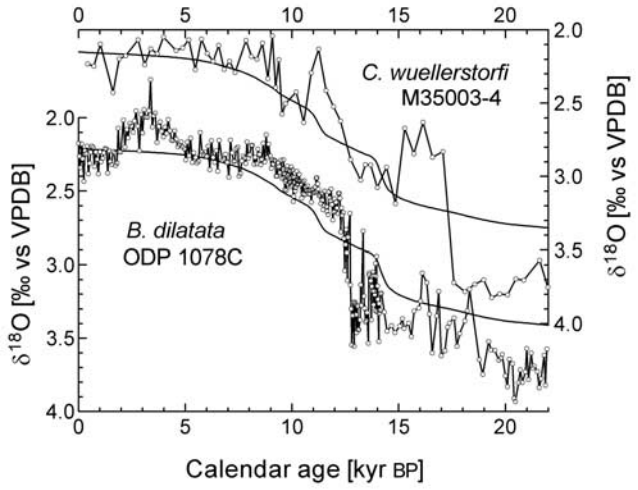

Figure 3. Oxygen isotope records of the benthic foraminifera *Cibicidoides wuellerstorfi* [*Hüls*, 2000] and *Bolivina dilatata* from sediment cores M35003-4 and ODP1078C, respectively. The solid lines denote the global $\delta^{18}O$ change [*Fairbanks*, 1989; *Fairbanks et al.*, 1992], plotted together with the benthic $\delta^{18}O$ data by matching the records in the late Holocene.

and Paul, 2001] is implemented for the advection of temperature and salinity [*Prange et al.*, 2003]. Depth-dependent horizontal and vertical diffusivities are prescribed ranging from 10^3 m^2 s^{-1} at the surface to 0.5×10^3 m^2 s^{-1} at the bottom, and from 0.6×10^{-4} m^2 s^{-1} to 1.3×10^{-4} m^2 s^{-1}, respectively. A bottom boundary layer formulation is included to improve the representation of overflows [*Lohmann*, 1998]. In order to close the hydrological cycle, a runoff scheme transports freshwater from the continents to the ocean. We carried out two experiments, one with present-day conditions and a second with glacial conditions. To drive the ocean in the present-day experiment, monthly fields of wind stress, surface air temperature, and freshwater flux are taken from the control integrations of the atmospheric general circulation model ECHAM3/T42 [*Roeckner et al.*, 1992; *Lohmann and Lorenz*, 2000]. For the surface heat flux Q we use a boundary condition of the form

$$Q = \left(\lambda_1 - \lambda_2 \nabla^2\right)(T_a - T_s), \qquad (1)$$

as suggested by *Rahmstorf and Willebrand* [1995]. Here T_a is the prescribed air temperature, and T_s denotes the ocean surface temperature. Unlike conventional temperature restoring, the thermal boundary condition (1) allows for scale selective damping of surface temperature anomalies. For the parameters λ_1 and λ_2 we choose 15 W m^{-2} K^{-1} and 2×10^{12} W K^{-1}, respectively. This choice enables the simulation of observed sea-surface temperatures as well as the maintenance of large-scale temperature anomalies in the North Atlantic during meltwater perturbation experiments [*Prange et al.*, 2003]. The hybrid-coupled model approach has been successfully employed in previous paleostudies [*Prange et al.*, 2002; *Knorr and Lohmann*, 2003; *Romanova et al.*, 2004]. The main advantage of this approach is that paleoceanographic observations can directly be "assimilated" into the model.

[11] For the glacial experiment the ECHAM3/T42 model was forced with *Climate: Long Range Investigation, Mapping, and Prediction* (*CLIMAP*) *Project Members*, [1981] sea-surface temperatures, with an additional cooling of 3°C for the tropical ocean between 30°S and 30°N [*Lohmann and Lorenz*, 2000]. The 3°C tropical cooling relative to *CLIMAP Project Members* [1981] provides a consistent picture of the LGM climate, concerning the hydrological cycle and annual mean surface temperatures [*Lohmann and Lorenz*, 2000] as well as the mean temperature of the coldest month and glacial snow lines (S. Lorenz and G. Lohmann, Reconciling snowlines with tropical sea-surface temperatures during the Last Glacial Maximum, submitted to *Geochemistry*, *Geophysics*, *Geosystems*, 2003). Changes in insolation, atmospheric carbon dioxide concentration, and ice sheet distributions are taken into account. In all model components the ice age paleotopography of *Peltier* [1994] is applied along with a global sea level drop of 120 m. The model was integrated into equilibrium for both climatic situations (5000 years of model integration). Afterward, these equilibria were perturbed by a meltwater influx of 0.15 Sv into the North Atlantic between 40°N and 55°N, lasting 500 years.

3. Results

3.1. Paleoclimatic Records

[12] The $\delta^{18}O$ records of *C. wuellerstorfi* (M35003-4) and *B. dilatata* (ODP 1078C) show average glacial-interglacial amplitudes of ~1.6‰ (Figure 3). Core M35003-4 exhibits two large steps of ~0.9‰, a very steep one at 17 kyr occurring between two consecutive samples (300 and 295 cm), and a more gradual $\delta^{18}O$ decrease starting at 13 kyr. These pronounced shifts in $\delta^{18}O$ are coeval with the onsets of Heinrich event H1 and the Younger Dryas. ODP core 1078C likewise shows a prominent decrease in $\delta^{18}O$ of 0.9‰ at 13 kyr and some oscillations of 0.4–0.5‰ between 19 and 16 kyr and at 14 kyr. A prominent Holocene $\delta^{18}O$ decrease of 0.3‰ occurred between 5 and 2 kyr.

3.2. Climate Model Simulations for Present-Day and Glacial Background States

[13] Figure 4a shows the equilibrium temperature distributions in the Atlantic basin for present-day conditions and Figure 4b shows the glacial anomalies. At intermediate depths the glacial cooling relative to present-day conditions amounts to 2–5°C; in the deep ocean it is around 2°C. For a detailed description of the surface hydrography we refer to *Romanova et al.* [2004]. In the glacial experiment the Atlantic meridional overturning circulation is 15–20% weaker than in the present-day run (Figure 5). This reduction is consistent with other model simulations for the climate of the Last Glacial Maximum [*Ganopolski et al.*, 1998; *Weaver et al.*, 1998; *Shin et al.*, 2003]. However, we note that results from coupled general circulation models are contradictory, ranging from almost vanishing NADW formation [*Kim et al.*, 2003] to a significant strengthening of

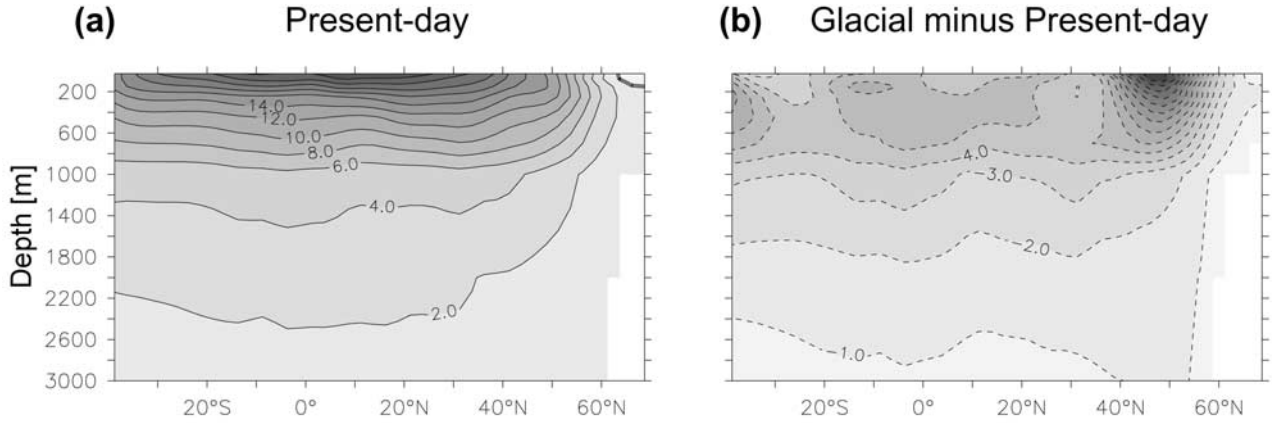

Figure 4. (a) Zonal mean Atlantic temperature simulated by the hybrid-coupled model under present-day conditions, contour interval is 2°C. (b) Simulated glacial anomaly, contour interval is 1°C.

the glacial NADW circulation compared to the present [*Hewitt et al.*, 2001; *Kitoh et al.*, 2001].

[14] In both experiments a North Atlantic freshwater flux perturbation of 0.15 Sv results in a complete breakdown of the THC (Figure 5). Under present-day conditions the net export of NADW to the Southern Ocean drops from ~8.5 to almost 0 Sv and does not recover after termination of the anomalous freshwater forcing. The THC settles into a new equilibrium, a so-called "off" mode. In contrast, the glacial conveyor starts to recover spontaneously as soon as the freshwater influx comes to an end. This monostable behavior of the glacial THC provides an explanation for THC recovery despite massive freshening in the North Atlantic during glacial times [*Ganopolski and Rahmstorf*, 2001; *Prange et al.*, 2002; *Romanova et al.*, 2004].

[15] Disturbing the THC causes a redistribution of heat in the Atlantic basin. Figure 6a displays the response of the temperature field after 500 years of anomalous freshwater forcing for the present-day ocean. The upper layers show the well-known hemispheric seesaw with cooling in the Northern Hemisphere and warming in the Southern Hemisphere [*Crowley*, 1992; *Stocker et al.*, 1992; *Manabe and Stouffer*, 1997]. In the middepth Atlantic Ocean the temperature increase is more widespread, owing to the reduced ventilation by cold intermediate and deep waters in conjunction with downward mixing of heat from the thermocline. Warming is strongest around 400 m water depth between 10° and 25°S in the present-day experiment. A similar pattern has been obtained by *Rind et al.* [2001] using the GISS coupled atmosphere-ocean model. The warming at 60°N is related to the shutdown of convection leading to reduced heat loss to the atmosphere.

[16] For the glacial freshwater perturbation experiment the same general structure of the temperature response is apparent as in the present-day simulation, although the upper layer seesaw is somewhat less pronounced (Figure 6b). The strongest warming likewise occurs at middepths but further south than for the present-day experiment, between 20° and 40°S. At core locations M35003-4 and ODP 1078C the temperature increase is 0.6°C and 1.8°C, respectively.

4. Discussion

[17] The oxygen isotope composition of foraminiferal tests depends on both the $\delta^{18}O$ and the temperature of ambient seawater during calcification. Because the mean $\delta^{18}O$ of ocean water significantly changed during the deglaciation owing to the melting of continental ice and freshwater runoff, we corrected the benthic isotope records

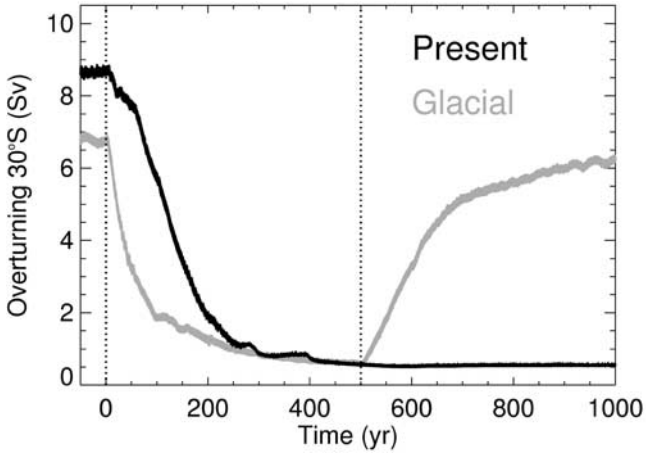

Figure 5. Temporal evolution of the Atlantic meridional overturning circulation in meltwater perturbation experiments under (a) present-day and (b) glacial conditions (the time series are filtered by 2-year running means). In the unperturbed state (before year zero) the overturning ratio, i.e., the ratio of NADW export to the Southern Ocean across 30°S (shown here) and maximum overturning in the North Atlantic, is about 0.75. A meltwater input of 0.15 Sv is applied to the North Atlantic between years 0 and 500. After termination of the anomalous freshwater forcing, the present-day THC remains in the "off" mode, whereas the glacial circulation recovers (monostability).

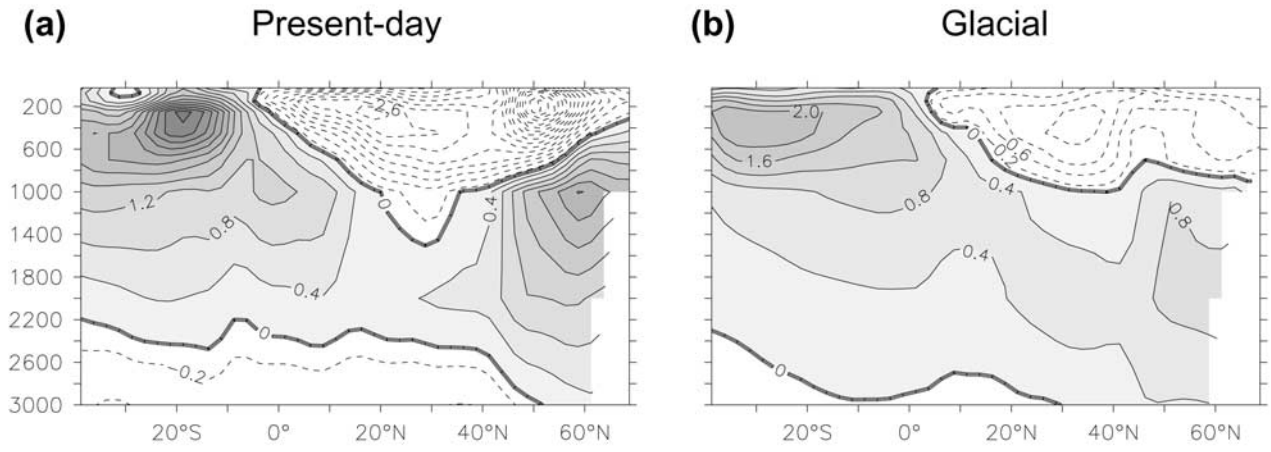

Figure 6. Response of the Atlantic Ocean to meltwater perturbations: (a) Zonally averaged temperature change at year 500 (end of meltwater perturbation) relative to the unperturbed equilibrium state for present-day conditions. (b) Same as in Figure 6a but for glacial conditions. Contour interval is 0.4°C; dashed lines represent cooling.

by subtracting the global $\delta^{18}O$ ice effect [*Fairbanks*, 1989; *Fairbanks et al.*, 1992] (heavy lines in Figure 3). The residual $\delta^{18}O$ curves ($\Delta\delta^{18}O$) exhibit pronounced excursions at 18 kyr, at the beginning of Heinrich event H1 (17 kyr), and at the Younger Dryas (13 kyr) (Figures 7f and 7g).

[18] The $\Delta\delta^{18}O$ shifts either reflect an increase in temperature, local changes in the oxygen isotope composition of seawater ($\delta^{18}O_w$), or a combination of $\delta^{18}O_w$ and temperature. A decrease of $\delta^{18}O_w$ in the range of 0.5 to 0.9‰ seems unlikely since both core sites are remote from any direct influence of isotopically light meltwater. In the freshwater perturbation experiment of the glacial ocean, we found a salinity decrease around 0.2 psu at the location of core M35003-4 (Figure 8) and hence estimate that the reduction of $\delta^{18}O_w$ did not exceed 0.1‰, given a slope of the $\delta^{18}O_w$: salinity relationship of 0.5 [*Broecker*, 1986] (or at most 0.2‰, if a slope of 1 is used which would be more appropriate for a region indeed affected by meltwater with a $\delta^{18}O$ value of −30 to −40‰). The modeled salinity change at the position of ODP core 1078C is around zero. Consequently, the major portion of the benthic $\delta^{18}O$ shifts in both cores M35003-4 and ODP 1078C at the beginning of Heinrich event H1 and the Younger Dryas should be explained by a rapid warming of 1–3°C when a decrease in $\delta^{18}O_c$ of 0.22‰ per 1°C temperature increase is assumed. The inaccuracy of the age model of both the global $\delta^{18}O$ curve and our benthic records, which in each case amounts to a few hundred years, does not significantly bias the estimated range of warming since the variations of the global $\delta^{18}O$ curve are low compared with the rapid $\delta^{18}O$ excursions at Heinrich event H1 and the Younger Dryas (Figure 3). Our results on middepth temperature change are consistent with benthic foraminiferal $\delta^{18}O$ records from the northeastern Brazilian continental slope at water depths of 767 m (3°40′ S) and 1090 m (21°37′ S) and the tropical African continental slope at 1502 m (6°23′ S), which show similar temperature increases during Heinrich event H1 and the Younger Dryas [*Arz et al.*, 1999; *Mulitza and Rühlemann*, 2000].

[19] A comparison of our intermediate depth temperature reconstructions (Figures 7f and 7g) with high-resolution records of Greenland ice core oxygen isotopes [*Stuiver and Grootes*, 2000] (Figure 7a), ice-rafted debris [*Bond et al.*, 1999] (Figure 7b), and sea-surface salinity [*Duplessy et al.*, 1992] (Figure 7c) from the northern North Atlantic, atmospheric radiocarbon derived from sediments of Lake Suigetsu, Japan [*Kitagawa and van der Plicht*, 2000] (Figure 7d), and Cd/Ca ratios in benthic foraminiferal tests from the Bermuda Rise [*Boyle and Keigwin*, 1987] (Figure 7e) indicates that the shifts in $\delta^{18}O$ of the tropical Atlantic are associated with freshening of the northern North Atlantic, abrupt changes in the rate of Atlantic thermohaline overturning, and cooling of the atmosphere over Greenland. Variations in the amount of ice-rafted debris (Figure 7b) indicate changes in freshwater flux to the North Atlantic owing to iceberg discharge from the adjacent continents with large increases during Heinrich event H1 and the Younger Dryas [*Bond et al.*, 1999], periods when sea-surface salinity in the North Atlantic decreased significantly (Figure 7c) as inferred from temperature estimates based on foraminiferal assemblages and $\delta^{18}O$ of planktic foraminifera [*Duplessy et al.*, 1992]. The record of $\Delta^{14}C_{atm}$ (Figure 7d) is a function of the production rate of ^{14}C in the upper atmosphere and the sizes of and exchange rates between the major carbon reservoirs. North Atlantic Deep Water is presently the major source of ^{14}C to the deep sea, and changes in the strength of this water mass probably dominate the variations in $\Delta^{14}C_{atm}$ [*Clark et al.*, 2002]. Positive anomalies in the $\Delta^{14}C_{atm}$ record hence largely reflect reduction in NADW formation and thermohaline overturning. The Cd/Ca maxima during Heinrich event H1 and the Younger Dryas likewise indicate a significant slowdown of NADW formation during these periods. Cd/Ca ratios of benthic foraminifera (Figure 7e)

trace deep water nutrient variability, which is linked to changes in water mass contributions from low-nutrient (low Cd/Ca) North Atlantic and high-nutrient (high Cd/Ca) Southern Ocean sources [*Boyle and Keigwin*, 1987]. The abrupt $\delta^{18}O$ decrease preceding Heinrich event H1 at 18 kyr, recorded in ODP 1078C (Figure 7f), may be related to a meltwater event which is not resolved in the other proxy records shown here; there is, however, evidence for smaller precursors to Heinrich events [*Bond et al.*, 1999].

[20] Both model and paleoclimatic data consistently show a middepth warming during THC slowdown. The amplitude of the warming in the model, however, seems to be slightly less compared to data (Figure 6b), which could either be interpreted as a model deficiency or data inaccuracy, or as the difficulty in interpreting the $\delta^{18}O$ signal. The model setup is admittedly simplified, so the underestimated warming may be attributed to missing feedbacks and simplified physics in the model. However, meltwater scenarios with fully coupled general atmosphere-ocean circulation models [*Manabe and Stouffer*, 1997; *Rind et al.*, 2001; *Lohmann*, 2003] show similar temperature anomalies. The benthic $\Delta\delta^{18}O$ signal is superimposed by a long-term warming trend from glacial to Holocene climate conditions. A deglacial Southern Ocean sea ice retreat [*Shemesh et al.*, 2002] during the Southern Hemisphere warming may lead to a resumption of the Atlantic conveyor circulation from weak glacial to strong interglacial THC conditions [*Knorr and Lohmann*, 2003] which may transform the southern warming globally. When subtracting this ''background warming'' at the end of the deglaciation, an intermediate depth warming of about 1°C during times of reduced overturning circulation is consistent with our paleoclimatic data (Figure 7) and model results (Figure 6). Furthermore, the deglacial temperature signal of ODP core 1078C may be influenced by changes in thermocline ventilation and preformed temperatures of Southern Ocean water masses supplied to the core location. The thermocline waters off Angola are currently fed by a mixture of Indian Ocean water and central water originating from the Subtropical Front [*Tomczak and Godfrey*, 1994]. Climate model experiments show that during the LGM the proportion of cool Southern Ocean water masses increased at the expense of warm Indian Ocean waters [*Paul and Schäfer-Neth*, 2003]. Hence a deglacial warming of the thermocline source waters may possibly cause an overestimation of the tropical Atlantic middepth warming related to the slowdown of NADW formation.

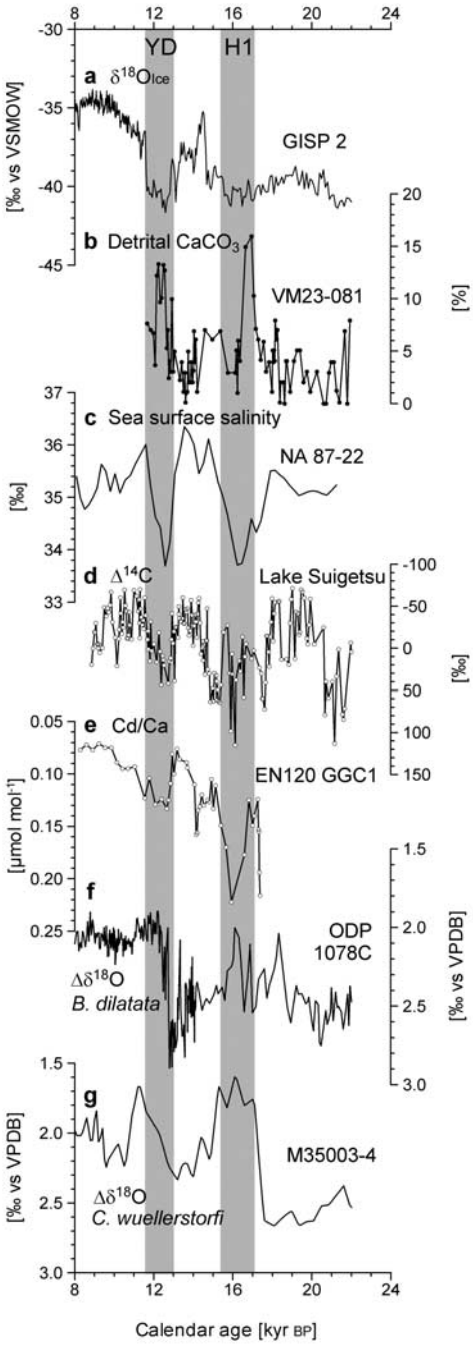

Figure 7. Climatic evolution of the last deglaciation in the tropical and northern Atlantic Ocean as indicated by proxy records of surface, intermediate, and deep water conditions. Shown is a comparison of the ice volume corrected oxygen isotope records of the benthic foraminifera *B. dilatata* (f) and *C. wuellerstorfi* (g) [*Hüls*, 2000] from sediment cores ODP 1078C (11°55′ S, 13°24′ E; 426 m water depth) and M35003-4 (12°05′ N, 61°15′ W; 1299 m water depth), respectively, indicating tropical Atlantic intermediate depth temperatures, with (a) oxygen isotopes from the GISP2 ice core (72°36′ N, 38°30′ W). [*Stuiver and Grootes*, 2000] indicating air temperatures over central Greenland, (b) detrital carbonate from North Atlantic sediment core VM23-081 (54°16′ N, 16°51′ W; 2393 m water depth) [*Bond et al.*, 1999], (c) sea-surface salinity from sediment core NA87-22 (55°30′ N, 14°42′ W, 2161 m water depth) from the Rockall Plateau [*Duplessy et al.*, 1992], (d) atmospheric radiocarbon from sediments of Lake Suigetsu, Japan [*Kitagawa and van der Plicht*, 2000; adapted from *Clark et al.*, 2002], and (e) cadmium/calcium ratios of benthic foraminiferal tests in sediment core EN120 GGC1 (33°40′ N, 57°37′ W, 4450 m) from the Bermuda Rise [*Boyle and Keigwin*, 1987]. H1 and YD denote Heinrich event H1 and the Younger Dryas period, respectively.

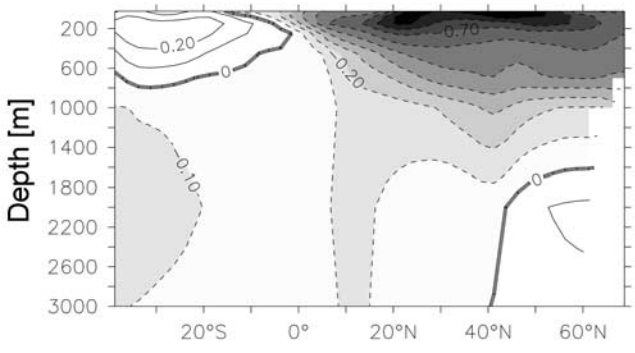

Figure 8. Response of the Atlantic salinity field to the meltwater perturbation under glacial conditions. Shown is the zonally averaged salinity change at year 500 (end of meltwater perturbation) relative to the unperturbed equilibrium state. Contour interval is 0.1 psu; dashed lines represent freshening.

[21] Both benthic $\Delta\delta^{18}O$ records show a warming at about 9 kyr (Figures 6f and 6g), coeval with a reduction in sea-surface salinity as obtained from core NA 87-22 proxy data (Figure 6c). Moreover, the benthic $\delta^{18}O$ record of ODP core 1078C and the salinity reconstruction from the Rockall Plateau [*Duplessy et al.*, 1992] reveal a close covariation over the entire Holocene interval with low $\delta^{18}O$ values (increased temperatures) off Angola corresponding to low salinities in the subpolar North Atlantic (Figure 9). We note that the reconstruction of sea-surface salinity from foraminiferal $\delta^{18}O$ critically depends on an independent SST estimate [*Wolff et al.*, 1999; *Schmidt*, 1999]. A recent SST reconstruction for core NA 87-22, based on the revised analogue method [*Waelbroeck et al.*, 2001], shows Holocene temperatures that deviate from those given by *Duplessy et al.* [1992], who used the Imbrie-Kipp transfer function method. Sea-surface salinities based on the data set of *Waelbroeck et al.* [2001] would thus differ from the curve shown in Figure 9. However, taking the salinities shown in Figure 9 at face value, the covariation of increased middepth temperatures off Angola and low sea-surface salinities in the subpolar North Atlantic suggests that small changes in THC (compared to Heinrich events) might be related to middepth warming in the tropical Atlantic during the Holocene period as well. The results from our present-day model experiment indicate that these processes could operate in the modern ocean in a similar way. We thus may speculate that the tropical Atlantic middepth warming signature provides a sensitive indicator of THC slowdown also for future climate change.

5. Conclusions and Outlook

[22] Our benthic isotope records and climate model simulations consistently suggest that a breakdown of the Atlantic overturning circulation was accompanied by rapid and intense warming of the intermediate depth tropical Atlantic and that this increase of temperature is a persistent feature during glacial and interglacial climate state. Changes in atmospheric moisture transports as a possible response to increased greenhouse gas forcing may have a similar effect as the deglacial meltwater discharges into the northern North Atlantic. Even though model predictions of future THC slowdown have not arrived at a consensus yet, most simulations of the ocean in a climate with increasing atmospheric greenhouse-gas concentrations predict a weakening of thermohaline circulation in the North Atlantic as the subpolar seas become warmer and fresher owing to enhanced precipitation and freshwater runoff from adjacent continents [*Manabe and Stouffer*, 1992; *Dixon et al.*, 1999; *Wood et al.*, 1999; *Cubasch et al.*, 2001]. However, the possible response for the next 100 years is rather uncertain: in some models the THC remains almost constant [*Latif et al.*, 2000; *Gent*, 2001]. This uncertainty is likely due to model differences in climate sensitivity, in the response of the hydrological cycle, and in the representation of processes and feedbacks, indicating that the strength of stabilizing and destabilizing feedbacks influencing the THC is still largely unknown. The strong relationship between the strength of the THC and tropical Atlantic intermediate depth temperatures may thus be highly relevant for tracing present-day and future changes of the THC. Recent oceanographic observations provoke the question whether THC weakening is already under way. Analyzing long-term hydrographic records, *Dickson et al.* [2002] showed that the headwaters of NADW have steadily become less saline over the past four decades, while the Faroe Bank channel overflow, one of the main contributors to the deep waters of the North Atlantic, concurrently declined by at least 20% relative to 1950 [*Hansen et al.*, 2001]. Akin to the ocean-

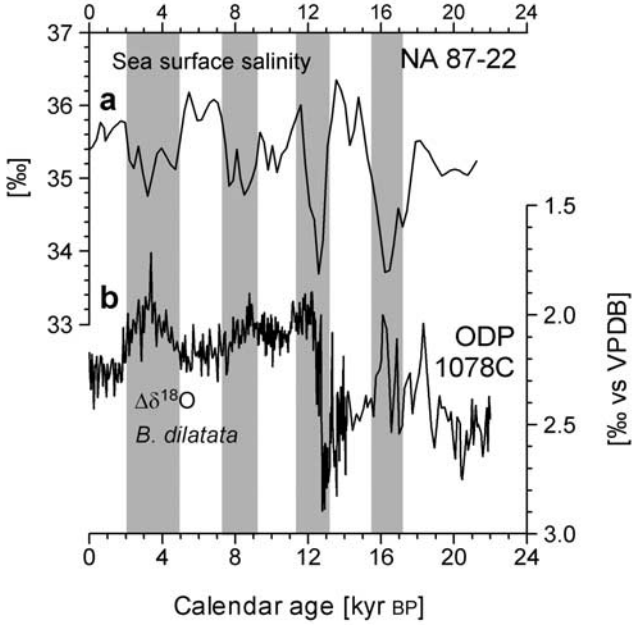

Figure 9. Comparison of the ice volume corrected oxygen isotope record of the (b) benthic foraminifera *B. dilatata* with (a) the sea-surface salinity record reconstructed from sediment core NA87-22 (55°30′ N, 14°42′ W, 2161 m water depth) from the Rockall Plateau [*Duplessy et al.*, 1992].

ographic processes during the last deglaciation, it is conceivable that a slowing of the THC should be accompanied by warming of tropical Atlantic intermediate depth waters. Using section data from the last 50 years in the tropical-subtropical Atlantic Ocean, *Arbic and Owens* [2001] indeed revealed a considerable warming trend of 0.5°C century^{-1} between 1000 and 2000 m water depth.

[23] The oxygen isotope data of the high-resolution ODP core 1078C suggest temperature increases of 0.8°C century^{-1} and 0.7°C century^{-1} at the onset of Heinrich event H1 and the Younger Dryas (averaged between 12.9 and 12.2 kyr), respectively; values comparable to the rate of 0.5°C at which the modern middepth Atlantic warms. We thus argue that the rates of temperature change of intermediate depth waters at Heinrich event H1 and the Younger Dryas provide a benchmark against which to assess warming rates in the 20th century as well as in the future. A primary objective of several climate research programs (e.g., RAPID, UK) is the design of practical strategies for monitoring climate variability and THC changes, which has shown to be one of the most uncertain factors of possible future climate shifts [*Cubasch et al.*, 2001; *Knutti et al.*, 2002]. The characteristic and pronounced pattern of temperature change in the Atlantic Ocean may aid in tracing for past, present, and future climate shifts associated with THC changes. The use of fingerprint techniques [e.g., *Hasselmann*, 1993] can increase the detectability of THC changes, provided that the middepth warming signal related to THC slowdown can be separated from the anthropogenic signal leading to surface warming in the formation area of the middepth water masses. For this purpose a large number of sites in the entire Atlantic must be included to determine the complete pattern of temperature gradient changes.

[24] **Acknowledgments.** We thank R. Schneider and M. Schulz for comments on an earlier version of the manuscript and G. Schmidt and an anonymous reviewer for their thorough reviews. P. Grootes and staff of the Leibniz-Labor in Kiel are acknowledged for providing AMS ^{14}C datings, and M. Segl, W. Bevern, and B. Meyer-Schack are acknowledged for performing the stable isotope measurements. This work was supported by the Bundesministerium für Bildung und Forschung (DEKLIM E and RASTA) and the Deutsche Forschungsgemeinschaft (Forschungszentrum Ozeanränder). Data are available from the PANGAEA database http://www.pangaea.de/home/cruehlemann).

References

Arbic, B. K., and W. B. Owens (2001), Climatic warming of Atlantic intermediate waters, *J. Clim.*, *14*, 4091–4108.

Arz, H., J. Pätzold, and G. Wefer (1999), The deglacial history of the western tropical Atlantic as inferred from high resolution stable isotope records off northeastern Brazil, *Earth Planet. Sci. Lett.*, *167*, 105–117.

Bard, E. (1988), Correction of accelerator mass spectrometry ^{14}C ages measured in planktonic foraminifera: Paleoceanographic implications, *Paleoceanography*, *3*, 635–645.

Bianchi, G. G., and I. N. McCave (1999), Holocene periodicity in North Atlantic climate and deep-ocean flow south of Iceland, *Nature*, *397*, 515–517.

Bond, G., W. Showers, M. Cheseby, R. Lotti, P. Almasi, P. deMenocal, P. Priore, H. Cullen, I. Hajdas, and G. Bonani (1997), A pervasive millennial-scale cycle in North Atlantic Holocene and glacial climates, *Science*, *278*, 1257–1266.

Bond, G. C., W. Showers, M. Elliot, M. Evans, R. Lotti, I. Hajdas, G. Bonani, and S. Johnson (1999), The North Atlantic's 1–2 kyr climate rhythm: Relation to Heinrich events, Dansgaard/Oeschger cycles and the Little Ice Age, in *Mechanisms of Global Climate Change at Millennial Time Scales*, edited by P. U. Clark, R. S. Webb, and L. D. Keigwin, pp. 35–58, AGU, Washington, D. C.

Bond, G., B. Kromer, J. Beer, R. Muscheler, M. N. Evans, W. Showers, S. Hoffmann, R. Lotti-Bond, I. Hajdas, and G. Bonani (2001), Persistent solar influence on North Atlantic climate during the Holocene, *Science*, *294*, 2130–2136.

Boyle, E. A., and L. Keigwin (1987), North Atlantic thermohaline circulation during the past 20,000 years linked to high-latitude surface temperature, *Nature*, *330*, 35–40.

Broecker, W. S. (1986), Oxygen isotope constraints on surface temperatures, *Quat. Res.*, *26*, 121–134.

Broecker, W. S. (1994), Massive iceberg discharges as triggers for global climate change, *Nature*, *372*, 421–424.

Butzin, M., M. Prange, and G. Lohmann (2003), Studien zur ^{14}C-Verteilung im glazialen Ozean mit einem globalen Ozeanmodell, *Terra Nostra*, *2003/6*, 86–88.

Charles, C. D., J. Lynch-Stieglitz, U. S. Ninnemann, and R. G. Fairbanks (1996), Climate connections between the hemisphere revealed by deep sea sediment core/ice core correlations, *Earth Planet. Sci. Lett.*, *142*, 19–27.

Clark, P. U., N. G. Pisias, T. F. Stocker, and A. J. Weaver (2002), The role of the thermohaline circulation in abrupt climate change, *Nature*, *415*, 863–869.

Climate: Long Range Investigation, Mapping, and Prediction (CLIMAP) Project Members (1981), *Seasonal Reconstruction of the Earth's Surface at the Last Glacial Maximum*, *Map and Chart Ser. MC-36*, Geol. Soc. Am., Boulder, Colo.

Crowley, T. C. (1992), North Atlantic Deep Water cools the Southern Hemisphere, *Paleoceanography*, *7*, 489–497.

Cubasch, U., et al. (2001), Projections of future climate change, in *Climate Change 2001: The Scientific Basis, Contribution of Working Group 1 to the Third Assessment Report of the Intergovernmental Panel on Climate Change*, edited by J. T. Houghton et al., pp. 881, Cambridge Univ. Press, New York.

deMenocal, P., J. Ortiz, T. Guilderson, and M. Sarnthein (2000), Coherent high- and low-latitude climate variability during the Holocene warm period, *Science*, *288*, 2198–2202.

Dickson, B., I. Yashayaev, J. Meincke, B. Turrell, S. Dye, and J. Holfort (2002), Rapid freshening of the deep North Atlantic Ocean over the past four decades, *Nature*, *416*, 832–837.

Dixon, K. W., T. L. Delworth, M. J. Spelman, and R. J. Stouffer (1999), The influence of transient surface fluxes on North Atlantic overturning in a coupled GCM climate change experiment, *Geophys. Res. Lett.*, *26*, 2749–2752.

Dunbar, R. B., and G. Wefer (1984), Stable isotope fractionation in benthic foraminifera from the Peruvian continental margin, *Mar. Geol.*, *59*, 215–225.

Duplessy, J. C., L. Labeyrie, M. Arnold, M. Paterne, J. Duprat, and T. C. E. Van Weering (1992), Changes in surface salinity of the North Atlantic Ocean during the last deglaciation, *Nature*, *358*, 485–488.

Fairbanks, R. G. (1989), A 17,000-year long glacio-eustatic sea level record: Influence of glacial melting rates on the Younger Dryas event and deep-ocean circulation, *Nature*, *342*, 637–642.

Fairbanks, R. G., C. D. Charles, and J. D. Wright (1992), Origin of global meltwater pulses, in *Radiocarbon After Four Decades*, edited by R. E. Taylor, pp. 473–500, Springer-Verlag, New York.

Ganopolski, A., and S. Rahmstorf (2001), Rapid changes of glacial climate simulated in a coupled climate model, *Nature*, *409*, 153–158.

Ganopolski, A., S. Rahmstorf, V. Petoukhov, and M. Claussen (1998), Simulation of modern and glacial climates with a coupled global climate model, *Nature*, *391*, 351–356.

Gent, P. R. (2001), Will the North Atlantic Ocean thermohaline circulation weaken during the 21st century?, *Geophys. Res. Lett.*, *28*, 1023–1026.

Hansen, B., W. R. Turrell, and S. Osterhus (2001), Decreasing overflow from the Nordic seas into the Atlantic Ocean through the Faroe

Bank channel since 1950, *Nature*, *411*, 927–930.

Hasselmann, K. (1993), Optimal fingerprints for the detection of time dependent climate change, *J. Clim.*, *6*, 1957–1971.

Hewitt, C. D., A. J. Broccoli, J. F. B. Mitchell, and R. J. Stouffer (2001), A coupled model study of the last glacial maximum: Was part of the North Atlantic relatively warm?, *Geophys. Res. Lett.*, *28*, 1571–1574.

Hughen, K. A., J. T. Overpeck, S. J. Lehman, M. Kashgarian, J. Southon, L. C. Peterson, R. Alley, and D. M. Sigman (1998), Deglacial changes in ocean circulation from an extended radiocarbon calibration, *Nature*, *391*, 65–68.

Hüls, C. M. (2000), Millennial-scale SST variability as inferred from Planktonic foraminiferal census counts in the western subtropical Atlantic, Ph.D. thesis, Christian Albrechts Univ., Kiel, Germany.

Hüls, M., and R. Zahn (2000), Millennial-scale sea surface temperature variability in the western tropical North Atlantic from planktonic foraminiferal census counts, *Paleoceanography*, *15*, 659–678.

Kim, S.-J., G. M. Flato, and G. J. Boer (2003), A coupled climate model simulation of the Last Glacial Maximum, part 2: Approach to equilibrium, *Clim. Dyn.*, *20*, 635–661.

Kitagawa, H., and J. van der Plicht (2000), Atmospheric radiocarbon calibration beyond 11,900 cal BP from Lake Suigetsu laminated sediments, *Radiocarbon*, *42*, 369–380.

Kitoh, A., S. Murakami, and H. Koide (2001), A simulation of the Last Glacial Maximum with a coupled atmosphere-ocean GCM, *Geophys. Res. Lett.*, *28*, 2221–2224.

Knorr, G., and G. Lohmann (2003), Southern Ocean origin for the resumption of Atlantic thermohaline circulation during deglaciation, *Nature*, *424*, 532–536.

Knutti, R., T. F. Stocker, F. Joos, and G.-K. Plattner (2002), Constraints on radiative forcing and future climate change from observations and climate model ensembles, *Nature*, *416*, 719–723.

Latif, M., E. Roeckner, U. Mikolajewicz, and R. Voss (2000), Tropical stabilisation of the thermohaline circulation in a greenhouse warming simulation, *J. Clim.*, *13*, 1809–1813.

Leonard, B. P. (1979), A stable and accurate convective modelling procedure based on quadratic upstream interpolation, *Comput. Methods Appl. Mech. Eng.*, *19*, 59–98.

Lohmann, G. (1998), The influence of a near-bottom transport parameterization on the sensitivity of the thermohaline circulation, *J. Phys. Oceanogr.*, *28*, 2095–2103.

Lohmann, G. (2003), Atmospheric and oceanic freshwater transport during weak Atlantic overturning circulation, *Tellus Ser. A*, *55*, 438–449.

Lohmann, G., and S. Lorenz (2000), On the hydrological cycle under paleoclimatic conditions as derived from AGCM simulations, *J. Geophys. Res.*, *105*, 17,417–17,436.

Lohmann, G., M. Butzin, K. Grosfeld, G. Knorr, A. Paul, M. Prange, V. Romanova, and S. Schubert (2003), The Bremen Earth System Model of Intermediate Complexity (BREMIC) designed for long-term climate studies: Model description, climatology, and applications, *Tech. Rep.*, Bremen Univ., Bremen. (available as http://www.palmod.uni-bremen.de/∼gerrit/BREMIC.html)

Maier-Reimer, E., U. Mikolajewicz, and K. Hasselmann (1993), Mean circulation of the Hamburg LSG OGCM and its sensitivity to the thermohaline surface forcing, *J. Phys. Oceanogr.*, *23*, 731–757.

Manabe, S., and R. J. Stouffer (1992), Century-scale effects of increased atmospheric CO_2 on the ocean-atmosphere system, *Nature*, *364*, 215–218.

Manabe, S., and R. J. Stouffer (1997), Coupled ocean-atmosphere model response to freshwater input: Comparison to Younger Dryas event, *Paleoceanography*, *12*(2), 321–336.

Mix, A. C., W. F. Ruddiman, and A. McIntyre (1986), Late Quaternary paleoceanography of the tropical Atlantic: 1. Spatial variability of annual mean sea-surface temperatures, 0–20,000 years BP, *Paleoceanography*, *1*, 43–66.

Mulitza, S., and C. Rühlemann (2000), African monsoonal precipitation modulated by interhemispheric temperature gradients, *Quat. Res.*, *53*, 270–274.

Oppo, D. W., L. D. Keigwin, and J. F. McManus (2001), Persistent suborbital climate variability in marine isotope stage 5 and termination II, *Paleoceanography*, *16*, 280–292.

Oppo, D. W., J. F. McManus, and J. L. Cullen (2003), Deepwater variability in the Holocene epoch, *Nature*, *422*, 277–278.

Paul, A., and C. Schäfer-Neth (2003), Modeling the water masses of the Atlantic Ocean at the Last Glacial Maximum, *Paleoceanography*, *18*(3), 1058, doi:10.1029/2002PA000783.

Peltier, W. R. (1994), Ice age paleotopography, *Science*, *265*, 195–201.

Poore, R. Z., H. J. Dowsett, S. Verardo, and T. M. Quinn (2003), Millennial- to century-scale variability in Gulf of Mexico Holocene climate records, *Paleoceanography*, *18*(2), 1048, doi:10.1029/2002PA000868.

Prange, M., V. Romanova, and G. Lohmann (2002), The glacial thermohaline circulation: Stable or unstable?, *Geophys. Res. Lett.*, *29*(21), 2028, doi:10.1029/2002GL015337.

Prange, M., G. Lohmann, and A. Paul (2003), Influence of vertical mixing on the thermohaline hysteresis: Analyses of an OGCM, *J. Phys. Oceanogr.*, *33*, 1707–1721.

Rahmstorf, S., and J. Willebrand (1995), The role of temperature feedback in stabilizing the thermohaline circulation, *J. Phys. Oceanogr.*, *25*, 787–805.

Rind, D., G. L. Russell, G. A. Schmidt, S. Sheth, D. Collins, P. DeMenocol, and J. Teller (2001), Effects of glacial meltwater in the GISS coupled atmosphere-ocean model: 2. A bipolar seesaw in Atlantic Deep Water production, *J. Geophys. Res.*, *106*, 27,355–27,366.

Roeckner, E., et al. (1992), Simulation of the present-day climate with the ECHAM model: Impact of model physics and resolution, *MPI Rep. 93*, Max Planck Inst. für Meteorol., Hamburg, Germany.

Romanova, V., M. Prange, and G. Lohmann (2004), Stability of the glacial thermohaline circulation and its dependence on the background hydrological cycle, *Clim. Dyn.*, in press.

Rühlemann, C., S. Mulitza, P. M. Müller, G. Wefer, and R. Zahn (1999), Warming of the tropical Atlantic Ocean and slowdown of thermohaline circulation during the last deglaciation, *Nature*, *402*, 511–514.

Schäfer-Neth, C., and A. Paul (2001), Circulation of the glacial Atlantic: A synthesis of global and regional modeling, in *The Northern North Atlantic: A Changing Environment*, edited by P. Schäfer, W. Ritzrau, and M. Schlüter, pp. 441–462, Springer-Verlag, New York.

Schmidt, G. A. (1999), Error analysis of paleosalinity calculations, *Paleoceanography*, *14*, 422–429.

Schmiedl, G., A. Mackensen, and P. J. Müller (1997), Recent benthic foraminifera from the eastern South Atlantic Ocean: Dependence on food supply and water masses, *Mar. Micropaleontol.*, *32*, 249–287.

Shemesh, A., D. Hodell, X. Crosta, S. Kanfoush, C. Charles, and T. Guilderson (2002), Sequence of events during the last deglaciation in Southern Ocean sediments and Antarctic ice cores, *Paleoceanography*, *17*(4), 1056, doi:10.1029/2000PA000599.

Shin, S.-I., Z. Liu, B. Otto-Bliesner, E. C. Brady, J. E. Kutzbach, and S. P. Harrison (2003), A Simulation of the Last Glacial Maximum climate using the NCAR-CCSM, *Clim. Dyn.*, *20*, 127–151.

Stocker, T. F., and D. G. Wright (1996), Rapid changes in ocean circulation and atmospheric radiocarbon, *Paleoceanogaphy*, *11*, 773–796.

Stocker, T. F., D. G. Wright, and L. A. Mysak (1992), A zonally averaged coupled ocean-atmosphere model for paleoclimate studies, *J. Clim.*, *5*, 773–797.

Stuiver, M., and P. M. Grootes (2000), GISP2 oxygen isotope ratios, *Quat. Res.*, *53*, 277–284.

Stuiver, M., and P. J. Reimer (1993), Extended ^{14}C data base and revised CALIB 3.0 ^{14}C age calibration program, *Radiocarbon*, *35*, 215–230.

Stuiver, M., P. J. Reimer, E. Bard, W. Beck, G. S. Burr, K. A. Hughen, B. Kromer, G. McCormac, J. van der Plicht, and M. Spurk (1998), INTCAL98 radiocarbon age calibration, 24,000-0 cal BP, *Radiocarbon*, *40*, 1041–1083.

Tomczak, M., and J. S. Godfrey (1994), *Regional Oceanography: An Introduction*, Pergamon, New York.

Vidal, L., R. R. Schneider, O. Marchal, T. Bickert, T. F. Stocker, and G. Wefer (1999), Link between the North and South Atlantic during the Heinrich events of the last glacial period, *Clim. Dyn.*, *15*, 909–919.

Waelbroeck, A., J.-C. Duplessy, E. Michel, L. Labeyrie, D. Paillard, and J. Duprat (2001), The timing of the last deglaciation in North Atlantic climate records, *Nature*, *412*, 724–727.

Weaver, A. J., M. Eby, A. F. Fanning, and E. C. Wiebe (1998), Simulated influence of carbon dioxide, orbital forcing and ice sheets on the climate of the Last Glacial Maximum, *Nature*, *394*, 847–853.

Wolff, T., B. Grieger, W. Hale, A. Dürkoop, S. Mulitza, J. Pätzold, and G. Wefer (1999), On the reconstruction of paleosalinities, in *Use of Proxies in Paleoceanography: Examples From the South Atlantic*, edited by G. Fischer and G. Wefer, pp. 315–344, Springer-Verlag, New York.

Wood, R. A., A. B. Keen, J. F. B. Mitchell, and J. M. Gregory (1999), Changing spatial structure of the thermohaline circulation in response to atmospheric CO_2 forcing in a climate model, *Nature*, *399*, 572–575.

G. Lohmann, S. Mulitza, A. Paul, M. Prange, and G. Wefer, Universität Bremen, Fachbereich Geowissenschaften, Postfach 330 440, D-28334 Bremen, Germany. (gerrit@palmod.uni-bremen.de; smulitza@uni-bremen.de; apau@palmod.uni-bremen.de; mprange@palmod.uni-bremen.de; gwefer@uni-bremen.de)

C. Rühlemann, Bundesanstalt für Geowissenschaften und Rohstoffe, Referat Meeresgeologie, Postfach 51 01 53, D-30631 Hannover, Germany. (c.ruehlemann@bgr.de)